

# Hydrodynamic response in simulations within a multiphase transport model

De-Xian Wei and Xu-Guang Huang\*

*Department of Physics and Center for Field Theory and Particle Physics,  
Fudan University, Shanghai, 200433, China and*

*Key Laboratory of Nuclear Physics and Ion-beam Application (MOE), Fudan University, Shanghai 200433, China*

Li Yan†

*Department of Physics, McGill University 3600 rue University Montréal, QC Canada H3A 2T8*

We carry out simulations using a multiphase transport (AMPT) model to describe the observed flow signatures in  $\sqrt{s_{NN}} = 2.76$  TeV Pb-Pb collisions. Especially, we calculate the flow fluctuations of  $v_2$  in terms of cumulant ratios and the standardized skewness. Based on event-by-event AMPT simulations, we study the linear and cubic response relation between  $v_2$  and  $\varepsilon_2$ . We found that the observed response relation is compatible to what has been noticed in hydrodynamic modelings, with similar dependence on shear viscosity. Besides, this response relation is not sensitive to nonflow effects.

## I. INTRODUCTION

One remarkable achievement in high-energy heavy-ion experiments is the creation of a fluid-like quark-gluon system: the quark-gluon plasma (QGP). At energies available at the BNL Relativistic Heavy Ion Collider (RHIC) and the CERN Large Hadron Collider (LHC), it has been realized that the physics of the created QGP medium can be understood in terms of relativistic viscous hydrodynamics (see [1] for a recent review), with extremely small dissipative corrections. For instance, simulations based on hydrodynamic modelings of the QGP medium evolution provide so far the best description of the so-called harmonic flow  $V_n$ , and correlations and fluctuations of these flow [2–5], given an input of the specific shear viscosity (the ratio of shear viscosity to entropy density) close to a lower theoretical bound  $\eta/s = \hbar/4\pi k_B$  [6].

Harmonic flow  $V_n$  characterizes the azimuthal anisotropy of the generated particle spectrum in momentum space [7, 8]. For each collision event, with respect to the probability distribution of the generated particles in azimuthal angle,  $f(\phi_p)$ , one defines  $V_n$  as

$$V_n = v_n e^{in\Psi_n} \equiv \int \frac{d\phi}{2\pi} e^{in\phi_p} f(\phi_p). \quad (1)$$

The parameter  $n$  denotes harmonic order, with  $n = 2$  corresponding to elliptic flow,  $n = 3$  corresponding to triangular flow, etc. Note that  $V_n$  is a complex quantity by definition, which depends in principle on particle species, transverse momentum, pseudorapidity, etc. On an event-by-event basis, both its magnitude  $v_n$ , and phase  $\Psi_n$  fluctuate. Correlations and fluctuations of  $V_n$  determine all kinds of the measured flow signatures in experiments, such as the cumulants of flow and event-plane correlations [9].

Hydrodynamic modelings of heavy-ion collisions have led to a set of response relations between  $V_n$  and the fluctuating initial-state geometry of the colliding systems. More precisely, these relations are written in terms of initial state eccentricity  $\mathcal{E}_n$ , which is defined with respect to the initial-state energy density profile  $\rho(\vec{x}_\perp, \tau_0)$  as [10]

$$\mathcal{E}_n = \varepsilon_n e^{in\Phi_n} \equiv - \frac{\int d^2\vec{x}_\perp \rho(\vec{x}_\perp, \tau_0) r^n e^{in\phi}}{\int d^2\vec{x}_\perp r^n \rho(\vec{x}_\perp, \tau_0)}. \quad (2)$$

Note that, since  $|\mathcal{E}_n| = \varepsilon_n < 1$  by definition, harmonic flow  $V_n$  can be expanded with respect to  $\mathcal{E}_n$ , and a series of response relation can be obtained. A recent review on these response relations can be found in Ref. [11]. Although the response relation for  $V_2$  and similar response relations for higher order flow are empirical, based on event-by-event hydrodynamic simulations, they are conceptually compatible with the physics of hydrodynamic response theory. In particular, one may understand these response as evolution of long-wavelength hydrodynamic modes, in the way that the response coefficients solely depend on the medium dynamical properties. Therefore, in one selected centrality class where system multiplicity is roughly constant, fluctuations of these response coefficients can be ignored. In recent experiments, information on the flow correlations and fluctuations have been acquired with high precision, from which, hydrodynamic response relations can be examined [12–15].

Although hydrodynamic response relations are well established in hydrodynamic modelings, it is of interest to analyze these relations beyond hydrodynamics. In particular, one notices that nonflow effects result in additional event-by-event fluctuations, which are not characterized

<sup>1</sup> For  $n = 1$ , the dipolar anisotropy is defined as

$$\mathcal{E}_1 = \varepsilon_1 e^{in\Phi_1} \equiv - \frac{\int d^2\vec{x}_\perp \rho(\vec{x}_\perp, \tau_0) r^3 e^{i\phi}}{\int d^2\vec{x}_\perp r^3 \rho(\vec{x}_\perp, \tau_0)}$$

\* huangxuguang@fudan.edu.cn

† li.yan@physics.mcgill.ca

in hydrodynamics. In this work, by simulations based on a multiphase transport (AMPT) model [16], we reexamine the hydrodynamic response relation between  $V_2$  and  $\mathcal{E}_2$ . This paper is organized as follows: In Section II we briefly describe the AMPT model and parameters used in the present simulations. Flow signatures are obtained correspondingly by correlating generated particles. In particular, fluctuations of  $v_2$  are studied in terms of flow cumulants. The hydrodynamic response relation for  $v_2$  is detailed in Section III, where we emphasize its dependence on shear viscosity and nonflow effects. Throughout this paper, our results and analyses are mostly obtained based on AMPT simulations with respect to Pb-Pb collisions at  $\sqrt{s_{NN}} = 2.76$  TeV at the LHC. Similar results of the recent  $\sqrt{s_{NN}} = 5.02$  TeV Pb-Pb collisions are presented in Appendix A. We will use natural unit  $k_B = c = \hbar = 1$ .

## II. AMPT AND HEAVY-ION COLLISIONS

The AMPT model is a hybrid model in which QGP evolution in heavy-ion collisions is described by parton scatterings [16]. In the AMPT model, the initial-state particle distributions are generated by the HIJING model [17]. For the current study, string melting is considered so that the produced hadrons from HIJING model are further converted into valence quarks and antiquarks. Right before parton scatterings, we record the generated energy density profile of the system  $\rho(\vec{x}, \tau_0)$ , as the initial state of medium evolution. Initial state eccentricities of each event are then calculated with respect to Eq. (2). Parton scatterings, and accordingly the space-time evolution of QGP, are determined via ZPC parton cascade model [18], with the differential cross section

$$\frac{d\sigma}{dt} \approx \frac{9\pi\alpha_s^2}{2(t-\mu^2)^2}. \quad (3)$$

In the above equation,  $\alpha_s$  is the strong coupling constant,  $t$  is the Mandelstam variable, and  $\mu$  is the screening mass in the partonic system. These parameters are adjustable according to colliding systems so that measurable quantities in experiments, such as total yields, elliptic flow  $v_2$ , and two-pion correlations, can be reproduced. For later convenience, we also notice the following relation [19],

$$\frac{\eta}{s} \approx \frac{3\pi}{40\alpha_s^2} \frac{1}{\left(9 + \frac{\mu^2}{T^2}\right) \ln\left(\frac{18+\mu^2/T^2}{\mu^2/T^2}\right) - 18}, \quad (4)$$

which allows one to estimate the specific shear viscosity  $\eta/s$  in terms of partonic differential cross section. Note that an increasing running coupling  $\alpha_s$  leads to smaller  $\eta/s$ . Equation (4) represents a temperature-dependent estimate, as long as screen mass  $\mu$  is not linear in temperature [20]. In this work, we shall consider a constant screening mass, which results in a rise of  $\eta/s$  when temperature decreases. In the AMPT model, quarks and

antiquarks combine to form hadrons via a spatial coalescence model when scatterings stop. The hadronic phase of the system evolves according to a relativistic transport model until hadrons freeze out.

Although in each single event only a finite number of particles are produced, the probability distribution of these particles in azimuthal angle  $f(\phi_p)$  can still be estimated, from which one can obtain the complex flow harmonics  $V_n$  using definition Eq. (1). This complex  $V_n$  in each event suffers from statistical uncertainty due to finite number effect. A more systematic way to calculate flow harmonics is to correlate particles from all events in one centrality class, as has been done in experiments. From two-particle correlations, one obtains  $v_n\{2\}$ . From

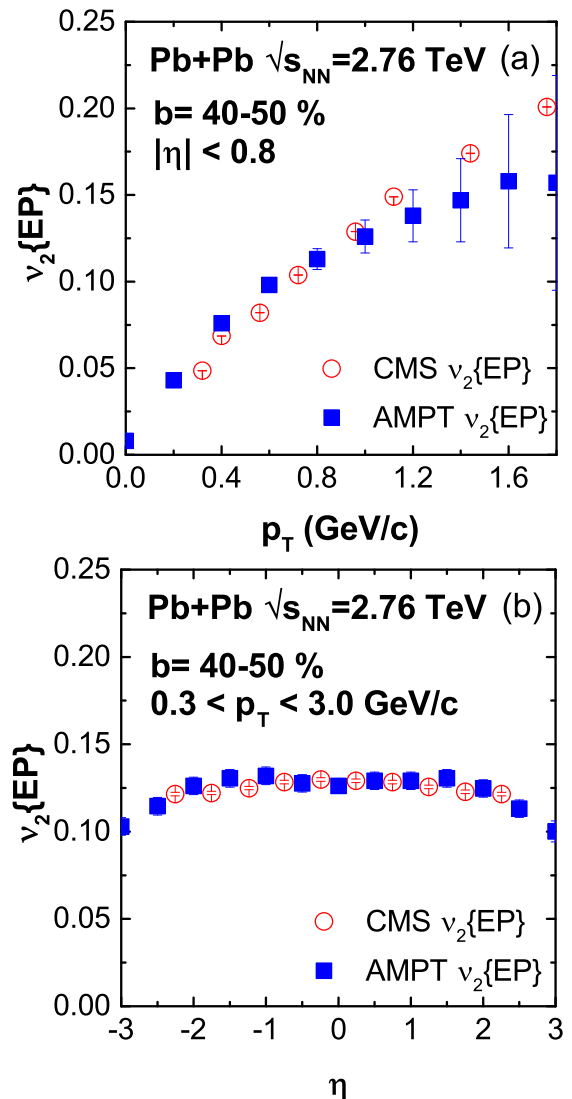


FIG. 1. (Color online) The (a)  $p_T$ - and (b)  $\eta$ - dependent elliptic flow  $v_2$  measured with respect to the event plane in the 40 - 50% centrality class. Blue symbols are obtained from AMPT simulations, in comparison with the CMS data at  $\sqrt{s_{NN}} = 2.76$  TeV [21].

four-, six-, and eight-particle correlations, one obtains higher order cumulants of flow harmonics:  $v_n\{4\}$ ,  $v_n\{6\}$  and  $v_n\{8\}$ . An estimate of the event plane in the collisions can be done in a similar manner, and correspondingly one has the flow harmonics measured with respect to the event plane  $v_n\{EP\}$ .

By choosing appropriate parameters in the AMPT model according to Ref. [19], we are able to reproduce the measured observables at the LHC. For instance, the differential elliptic flow  $v_2\{EP\}$  as a function of  $p_T$  and pseudorapidity are shown in Fig. 1 for the centrality class 40-50% of Pb-Pb collisions at  $\sqrt{s_{NN}} = 2.76$  TeV, with good agreements observed comparing to the CMS results. In these calculations, in addition to parameters that control the Lund string fragmentation,  $a = 0.5$  and  $b = 0.9$   $\text{GeV}^{-2}$ ,  $\alpha_s = 0.33$  and  $\mu = 3.2 \text{ fm}^{-1}$  are chosen, so that effectively one has a relatively large specific shear viscosity. At the initial temperature of LHC Pb-Pb collisions at  $\sqrt{s_{NN}} = 2.76$  TeV, which is around  $T \approx 468$  MeV obtained by estimating the initial energy density, one effectively has  $\eta/s = 0.273$  in the deconfined system.

In recent experiments at LHC energies, more sophisticated measurements of elliptic flow have been carried out, revealing the fluctuating nature of  $v_2$  (cf Ref. [22–24]). To estimate the fluctuation effect of  $v_2$ , for the Pb-Pb collisions at  $\sqrt{s_{NN}} = 2.76$  TeV, in each 5%-centrality bin from the 15% to 60%, we generate approximately 5000

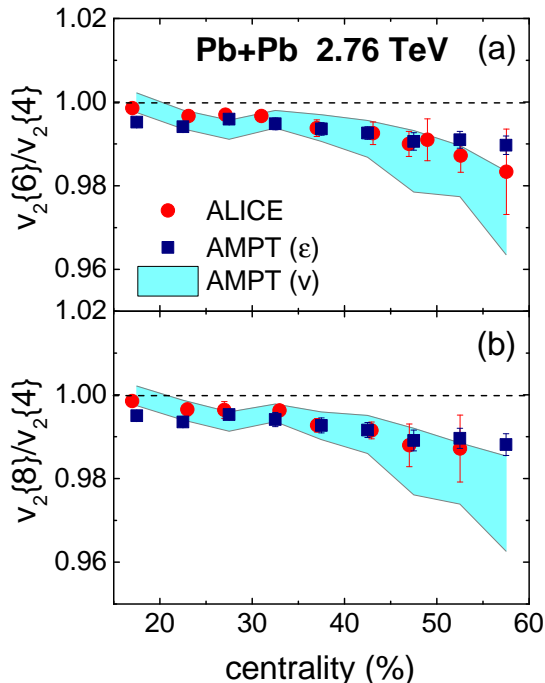


FIG. 2. (Color online) Ratios of cumulants (a)  $v_2\{6\}/v_2\{4\}$  and (b)  $v_2\{8\}/v_2\{4\}$ . Red points are from ALICE collaboration [22], colored bands are results of AMPT calculations. The corresponding cumulant ratios of initial ellipticity  $\varepsilon_2$  are shown as blue squares.

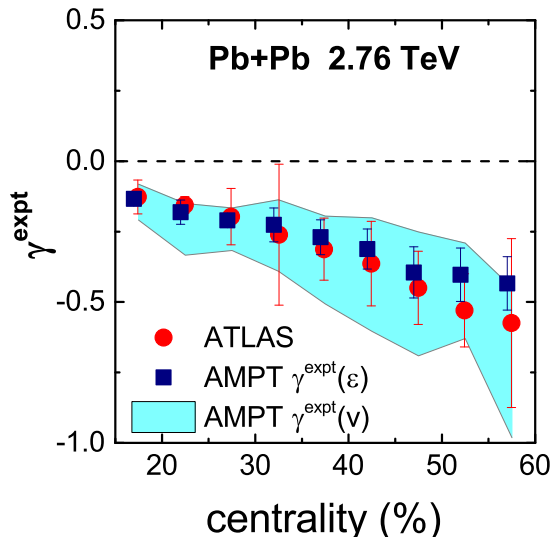


FIG. 3. (Color online) Standardized skewness of  $v_2$  fluctuations in Pb-Pb collisions as a function of centrality from AMPT simulations (colored band) and ATLAS [14] data (red points). The corresponding results of standardized skewness of initial state  $\varepsilon_2$  are shown as blue squares.

events from AMPT simulations. In Fig. 2, our AMPT results for the ratio of  $v_2\{6\}/v_2\{4\}$  and ratio  $v_2\{8\}/v_2\{4\}$  are presented as colored bands as a function of centrality percentile. The width of bands corresponds to statistical errors due to finite number effect, which in our calculations are estimated via a jackknife resampling. In comparison to the experiments from the ALICE Collaboration (red points), an overall agreement is observed within errors, which indicates that AMPT model is able to capture the non-Gaussian properties of  $v_2$  fluctuations.

One should be aware that both ratios are less than unity, and also the fact that  $v_2\{8\}$  is smaller than  $v_2\{6\}$ , are characteristic natures of flow fluctuations known from hydrodynamic modeling. In hydrodynamic modeling of heavy-ion collisions, fluctuations of elliptic flow  $v_2$  are mostly determined by fluctuations of initial ellipticity  $\varepsilon_2$ , due to the fact that  $V_2 \propto \mathcal{E}_2$ . This is also observed in our AMPT calculations. As shown in Fig. 2 the ratio of cumulants of  $\varepsilon_2$  (blue squares) are compatible with those of  $v_2$ , except for very peripheral collisions where the ratios of  $\varepsilon_2$  are slightly larger.

The information of  $v_2$  fluctuations can be as well captured by skewness. Given  $v_2\{2\}$ ,  $v_2\{4\}$  and  $v_2\{6\}$ , one may estimate the standardized skewness as [14]

$$\gamma^{expt} \equiv -6\sqrt{2}v_2\{4\}^2 \frac{v_2\{4\} - v_2\{6\}}{[v_2\{2\}^2 - v_2\{4\}^2]^{3/2}}. \quad (5)$$

Fig. 3 depicts the estimated standardized skewness of  $v_2$  fluctuations from our AMPT simulations, as colored bands. Again, the width of a band is determined by statistical errors via a jackknife resampling. AMPT results agree well with the recent experimental data (red points).

One observes a negative value of the skewness, with its magnitude increasing as centrality percentile grows. In hydrodynamic modeling, this negative skewness of  $v_2$  fluctuations is understood as a consequence of the negative skewness of  $\varepsilon_2$ , due to the combined effect of an upper bound  $\varepsilon_2 < 1$  and a nonzero mean of ellipticity in the reaction plane. Similarly, we notice that, in the case of AMPT simulations, skewness of  $v_2$  is comparable with that of initial  $\varepsilon_2$ .

### III. HYDRODYNAMIC RESPONSE RELATION IN AMPT

In the previous section we have seen  $v_2$  fluctuations from AMPT simulations, in terms of the cumulant of  $v_2$  from multiparticle correlations and standardized skewness. Especially, the fluctuations of  $v_2$  follow to a large extent the fluctuations of  $\varepsilon_2$ . This feature is very similar to what one would expect in a hydrodynamic modeling of heavy-ion collisions, in which a hydrodynamic response relation between  $V_2$  and  $\mathcal{E}_2$  has been established [25],

$$V_2 = \kappa_2 \mathcal{E}_2 + \kappa'_2 \varepsilon_2^2 \mathcal{E}_2 + \delta_2 \quad (6)$$

Equation (6) is achieved by regarding initial state eccentricity  $\varepsilon_n$  as small quantities, hence one may expand the complex quantities  $V_2$  in terms of  $\mathcal{E}_n$ . Owing to the condition of rotational symmetry, the leading-order term is a linear response proportional to  $\mathcal{E}_2$ , with  $\kappa_2$  the linear response coefficient determined by medium dynamical expansion. The next-leading-order contribution is of cubic order, and is dominantly determined by  $O(\varepsilon_2^3)$ . Apparently, the cubic-order contribution is not important unless  $\varepsilon_2$  becomes large, as in peripheral collisions. The quantity  $\delta_2$  in Eq. (6) describes additional event-by-event fluctuations, which affects the response relation on an event-by-event basis.

Although  $V_2$  fluctuates from event to event, as well as  $\mathcal{E}_2$ , both the linear response coefficient  $\kappa_2$  and cubic-order response coefficient  $\kappa'_2$  are considered constant in each centrality class. By minimizing the effect of additional fluctuations  $\delta_2$ , one solves  $\kappa_2$  and  $\kappa'_2$  [25],

$$\kappa_2 = \frac{\text{Re}(\langle \varepsilon_2^6 \rangle \langle V_2 \mathcal{E}_2^* \rangle - \langle \varepsilon_2^4 \rangle \langle V_2 \mathcal{E}_2^* \varepsilon_2^2 \rangle)}{\langle \varepsilon_2^6 \rangle \langle \varepsilon_2^2 \rangle - \langle \varepsilon_2^4 \rangle^2} \quad (7a)$$

$$\kappa'_2 = \frac{\text{Re}(-\langle \varepsilon_2^4 \rangle \langle V_2 \mathcal{E}_2^* \rangle + \langle \varepsilon_2^2 \rangle \langle V_2 \mathcal{E}_2^* |\varepsilon_2|^2 \rangle)}{\langle \varepsilon_2^6 \rangle \langle \varepsilon_2^2 \rangle - \langle \varepsilon_2^4 \rangle^2}, \quad (7b)$$

where bracket  $\langle \dots \rangle$  indicates average over events. Note that if one ignores contribution from the cubic-order response,  $\kappa_2$  in Eq. (7) reduces to

$$\kappa_2 = \frac{\text{Re} \langle V_2 \mathcal{E}_2^* \rangle}{\langle \varepsilon_2^2 \rangle} \quad (8)$$

One may check that a cubic-order correction reduces slightly the linear response coefficient, comparing Eq. (8) to Eq. (7).

Equation (6) in hydrodynamic modeling has been verified by event-by-event hydrodynamic simulations [5, 25, 26]. It is interesting to test the response relation in AMPT model. In the present setup of AMPT simulations for Pb-Pb collisions at  $\sqrt{s_{NN}} = 2.76$  TeV, we focus on the centrality class 45-50%. In hydrodynamic modeling, in 45-50% centrality class, both linear and nonlinear response are found important. We generate approximately 5000 events in our AMPT simulations. A scatter plot of  $v_2$  versus  $\varepsilon_2$  is obtained and is shown Fig. 4 (d). Each point in Fig. 4 (d) corresponds to one collision event. It is worth mentioning that the statistical uncertainty of  $v_2$  in each event due to finite multiplicity is not included, which would in principle lead to a smearing along  $v_2$  in Fig. 4. In Fig. 4 (d), these points distribute along a line, except for a slight tilde at large values of  $\varepsilon_2$  which implies nonlinearity. We find that a response relation between magnitudes derived from Eq. (6), describes well the trend,

$$v_2 = \kappa_2 \varepsilon_2 + \kappa'_2 \varepsilon_2^3, \quad (9)$$

similar to what one would expect from hydrodynamics. Given these solved values of  $\kappa_2$  and  $\kappa'_2$  according to Eq. (7), Eq. (9) is plotted in Fig. 4 (d) as the red solid line. Without the cubic-order correction, one has  $v_2 = \kappa_2 \varepsilon_2$  which is shown as white dashed line in the figure. It should be emphasized that the red line and white dashed line are *not* fitting the scattering points, but were determined with respect to the solved values of  $\kappa_2$  and  $\kappa'_2$  according to Eq. (7). Note also that the resulting linear response coefficient  $\kappa_2$  are not identical with or without cubic-order corrections. Dispersion around the linear and cubic-order response reflects event-by-event fluctuations. The width of the dispersion is related to fluctuation strength.

#### A. Effect of $\eta/s$

In hydrodynamics, the effects of  $\eta/s$  are twofold. First, it crucially determines medium response, *i.e.*,  $\kappa_2$  and  $\kappa'_2$ . When  $\eta/s$  increases, the linear response coefficient is suppressed. Second, from hydrodynamic simulations, it has also been noticed that event-by-event fluctuations around hydrodynamic response relations are reduced with respect to a larger value of  $\eta/s$  [5, 25].

To study the dissipative effect in AMPT simulations, by changing parameters for the parton cascade and for the Lund string fragmentation, we adjust effectively the ratio of shear viscosity to entropy density  $\eta/s$  of partons, with respect to Eq. (4). We simulate using the AMPT model in the same centrality class (45-50%), keeping total multiplicity unchanged but varying  $\eta/s$ . We summarize these four sets of parameters used in AMPT simulations in Table I. In addition to set D that has been used in previous sections to describe the  $\sqrt{s_{NN}} = 2.76$  TeV Pb-Pb collisions, which has, at  $T = 468$  MeV,  $\eta/s = 0.273$ , parameter set A, B, and C lead to, at  $T = 468$  MeV,

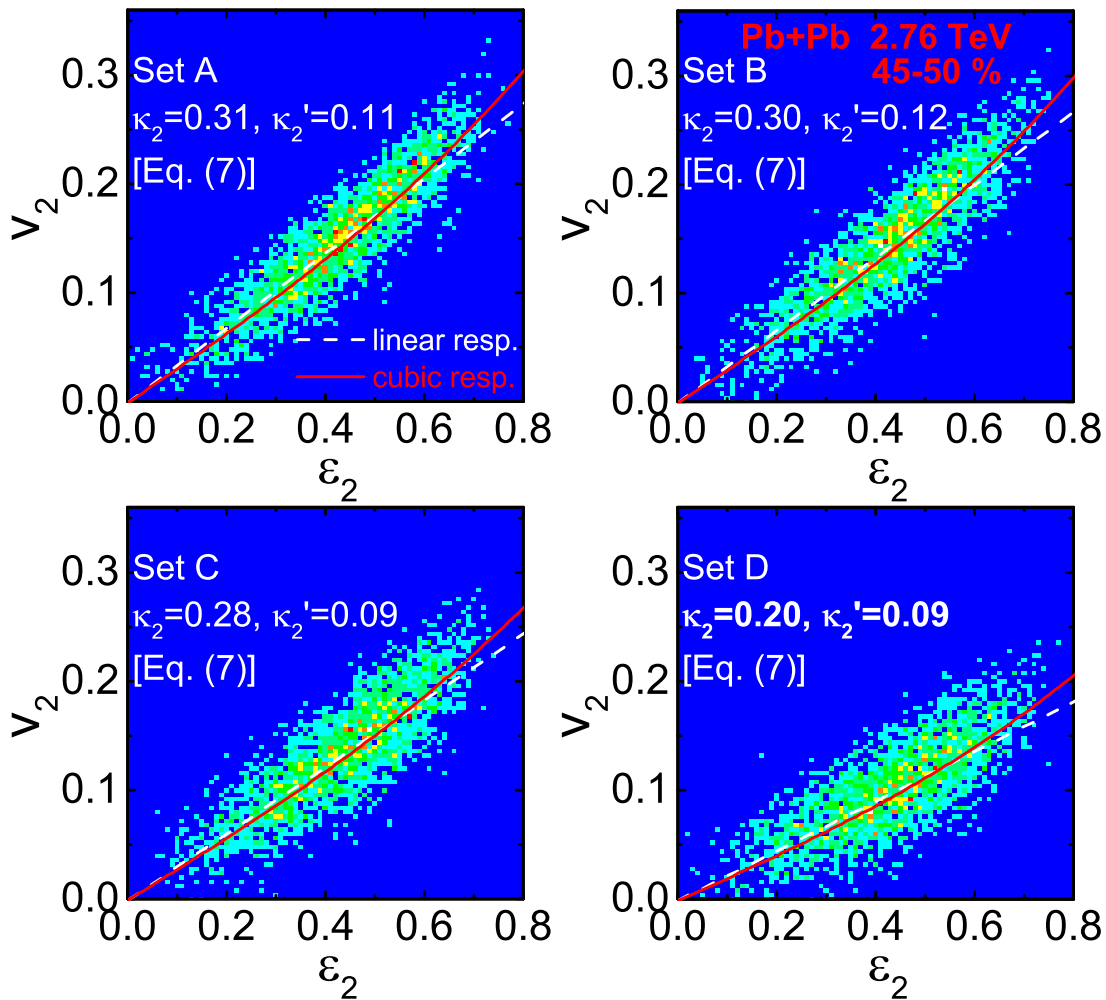


FIG. 4. (Color online) Scatter plot of event-by-event  $v_2$  from AMPT simulations for Pb-Pb collisions, as a function of  $\varepsilon_2$ . We take model parameters so that the effective specific shear viscosity  $\eta/s$  is increased from (a) 0.08, to (b) 0.10, (c) 0.14, and (d) 0.273, at temperature  $T = 468$  MeV. Red solid lines are from relation Eq. (9) with a cubic-order correction, while white dashed lines correspond to linear response relation.

TABLE I. Parameters used in AMPT simulations corresponding to different values of  $\eta/s$  at  $T = 468$  MeV. Parameters are taken according to Ref. [27, 28].

	Set			
	A	B	C	D
$\eta/s$ ( $T = 468$ MeV)	0.08	0.10	0.14	0.273
$a$	2.2	2.2	2.2	0.5
$b$ ( $\text{GeV}^{-2}$ )	0.5	0.5	0.5	0.9
$\alpha_s$	0.47	0.47	0.47	0.33
$\mu$ ( $\text{fm}^{-1}$ )	1.8	2.3	3.2	3.2

$\eta/s = 0.08, 0.10$  and  $0.14$  respectively. Correspondingly, results with respect to these simulations are shown in Fig. 4 (a), Fig. 4 (b) and Fig. 4 (c).

For each set of  $\eta/s$ , we calculate linear and cubic response coefficients,  $\kappa_2$  and  $\kappa_2'$ , giving rise to the response

relation with (red solid lines) or without (white dashed lines) cubic-order corrections. As anticipated, the value of linear response coefficient, the slope of lines in Fig. 4, is reduced as  $\eta/s$  increases, consistency with hydrodynamic modeling of heavy-ion collisions. We plot in Fig. 5 (a) the obtained value of linear and cubic response coefficients. The cubic-order response coefficient remains approximately constant,  $\kappa_2' \approx 0.1$ .

In contrast to hydrodynamic modeling, the event-by-event fluctuations are not suppressed by viscosity in the AMPT simulations, as can be seen from the width of dispersion in Fig. 4. In fact, one finds a slight increase of the fluctuation strength, if it is measured relative to the mean of  $v_2$ ,  $\langle |\delta_2|^2 \rangle / \langle v_2^2 \rangle$ . To quantify these effects, we measure the correlation of complex variables  $V_2$  and  $\varepsilon_2$ , by the Pearson correlation coefficient,

$$C(2, 2) = \frac{\text{Re} \langle V_2 \varepsilon_2^* \rangle}{\sqrt{\langle v_2^2 \rangle \langle \varepsilon_2^2 \rangle}}. \quad (10)$$

The Pearson correlation coefficient  $C(2,2)$  captures simultaneously correlation between magnitudes and phases. An absolute correlation is approached when  $C(2,2) = 1$ , while  $C(2,2) = 0$  indicates no correlation. Since fluctuations tend to break correlation between  $V_2$  and  $\mathcal{E}_2$ , the effect of fluctuation reduces  $C(2,2)$ . In Fig. 5 (b), we indeed find that  $C(2,2)$  decreases linearly as  $\eta/s$  increases from set A to set D.

### B. Nonflow subtraction

We have studied the linear and cubic response which relates elliptic flow  $V_2$  and initial ellipticity  $\mathcal{E}_2$  via AMPT simulations. Although the strategy is very similar to hydrodynamic simulations, with the linear and cubic-

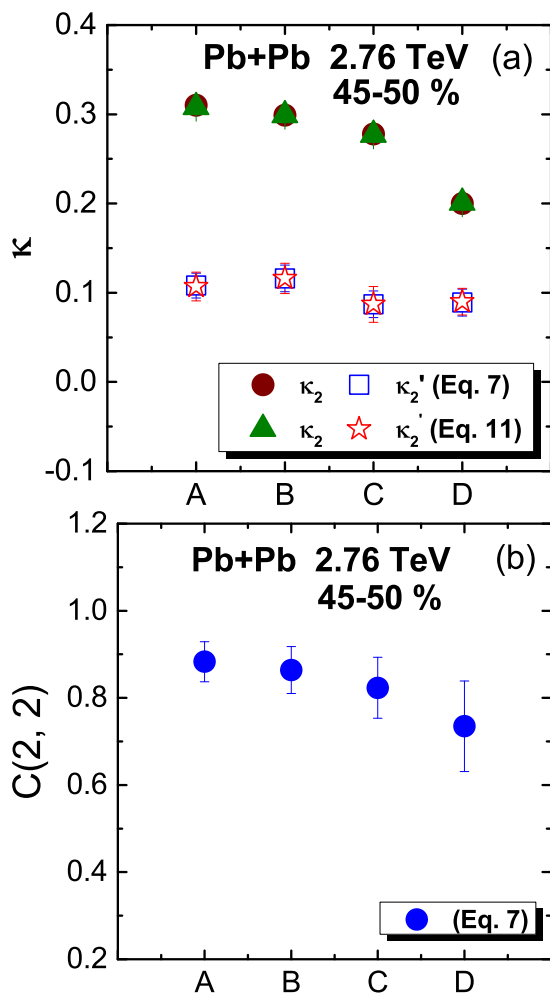


FIG. 5. (Color online) (a) AMPT results of the linear response and cubic response coefficients of the Pb-Pb 45-50% centrality class for four different sets of parameters corresponding to an increase of  $\eta/s$  from set A to set D, with respect to Eq. (7) and Eq. (11) with nonflow subtraction. (b) Pearson correlation coefficient  $C(2,2)$  for different sets of parameters.

order response coefficients obtained through minimizing event-by-event fluctuations, AMPT simulations contain nonflow effects. These nonflow effects are beyond pure hydrodynamic calculations, including, *e.g.*, short-ranged correlations in the deconfined medium from particle scatterings, hence they are nonhydrodynamic. Nonetheless, considering the fact that linear and cubic response relations are hydrodynamic and are dominated by the evolution of long-wavelength modes of the medium system, one would expect that the response relations depend little on nonflow effects.

In order to test the nonflow effects on the linear and cubic response, we subtract nonflow contributions in the AMPT simulations. To subtract nonflow effects in the flow harmonics, one may either take a pseudorapidity gap or rely on multiparticle cumulants. Both methods have been applied extensively in experiments [29–31]. Therefore, based on the response relation in Eq. (6), we find from the two-particle and four-particle correlations,

$$v_2\{2, |\Delta\eta|\} = \kappa_2 \varepsilon_2\{2\} \left[ 1 + \frac{\kappa_2' \langle \varepsilon_2^4 \rangle}{\kappa_2 \langle \varepsilon_2^2 \rangle} \right], \quad (11a)$$

$$v_2\{4\} = \kappa_2 \varepsilon_2\{4\} \left[ 1 + \frac{\kappa_2' 2 \langle \varepsilon_2^2 \rangle \langle \varepsilon_2^4 \rangle - \langle \varepsilon_2^6 \rangle}{\kappa_2 2 \langle \varepsilon_2^2 \rangle^2 - \langle \varepsilon_2^4 \rangle} \right]. \quad (11b)$$

In writing Eq. (11), we have assumed that a pseudorapidity gap is sufficient to take out the nonflow contribution, *i.e.*,  $\delta_2$ , in  $v_2\{2\}$ . In practice, a pseudorapidity gap

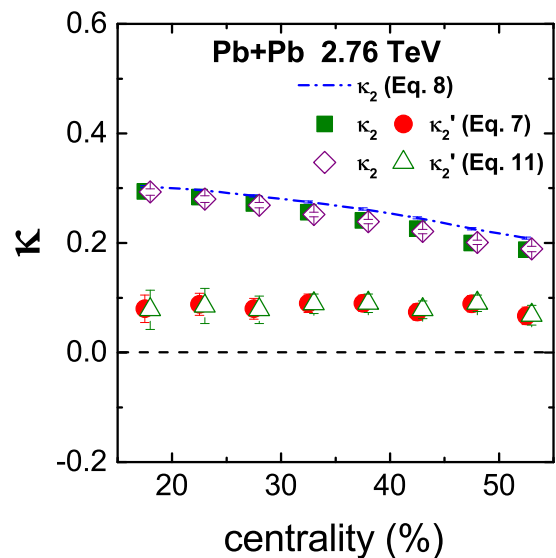


FIG. 6. (Color online) Linear and cubic-order response coefficients  $\kappa_2$  and  $\kappa_2'$  as a function of centrality percentile, from AMPT simulations of Pb-Pb collisions at  $\sqrt{s_{NN}} = 2.76$  TeV. The results of  $\kappa_2$  and  $\kappa_2'$  are calculated according to Eq. (7) and Eq. (11) corresponding to nonflow effects subtraction, respectively. For comparison, the linear response coefficient  $\kappa$  calculated with respect to Eq. (8) is shown as dashed line.

$|\Delta\eta| > 1$  is taken into account in our AMPT simulations for  $v_2\{2, |\Delta\eta|\}$ . Similarly,  $\delta_2$  does not appear in  $v_2\{4\}$ . Equation (11) then allows us to solve  $\kappa_2$  and  $\kappa'_2$ , without nonflow effects. The corresponding results of response coefficients are shown in Fig. 5 (a) as a function of  $\eta/s$ , and in Fig. 6 as a function of centrality percentile. As expected, numerical solutions of the response coefficients are found to be compatible with or without nonflow contributions.

#### IV. SUMMARY AND DISCUSSIONS

In this work, we have carried out AMPT simulations for Pb-Pb collisions at the LHC energy  $\sqrt{s_{NN}} = 2.76$  TeV. Our AMPT results of elliptic flow, especially the fluctuations of  $v_2$  are compatible with experiments. In addition, we found that the fluctuation behavior of  $v_2$ , characterized in terms of cumulant ratios or the standardized skewness, is closely related to that of  $\varepsilon_2$ . This feature has been noticed in hydrodynamic modelings, where the hydrodynamic response relations were proposed to explain the generation of harmonic flow. In the AMPT model, we observed very similar response relations, which can be well described by proper linear and cubic-order response coefficients. This observation confirms the fact that elliptic flow  $v_2$  is indeed a consequence of medium response to initial state  $\varepsilon_2$ . Since the medium response reflects long-wavelength mode evolution, which is hydrodynamic, similarity to what has been found in hydrodynamic modelings is understandable. However, AMPT simulations contain extra event-by-event fluctuations due to nonflow effects. Even though these fluctuations are nonhydrodynamic, as they are not sensitive to dissipative effect of the medium system, they do not affect the response relations.

#### ACKNOWLEDGMENTS

We thank Jean-Yves Ollitrault and Zi-Wei Lin for very helpful discussions. D.X.W. and X.G.H. are supported by the Young 1000 Talents Program of China, NSFC with Grant No. 11535012 and No. 11675041. L.Y. is supported in part by the Natural Sciences and Engineering Research Council of Canada.

#### Appendix A: AMPT RESULTS OF Pb-Pb COLLISIONS AT $\sqrt{s_{NN}} = 5.02$ TeV

Recent experiments at the LHC has reached  $\sqrt{s_{NN}} = 5.02$  TeV for Pb-Pb collisions, where the fluctuations of  $v_2$  have been measured. In this appendix, we present our results of  $v_2$  fluctuations in terms of cumulant ratios in Fig. 7 and the standardized skewness in Fig. 8, from AMPT simulations. In the AMPT simulations for  $\sqrt{s_{NN}} = 5.02$  TeV, we found that the parameter set D (see Table I) can be used to well describe the observed

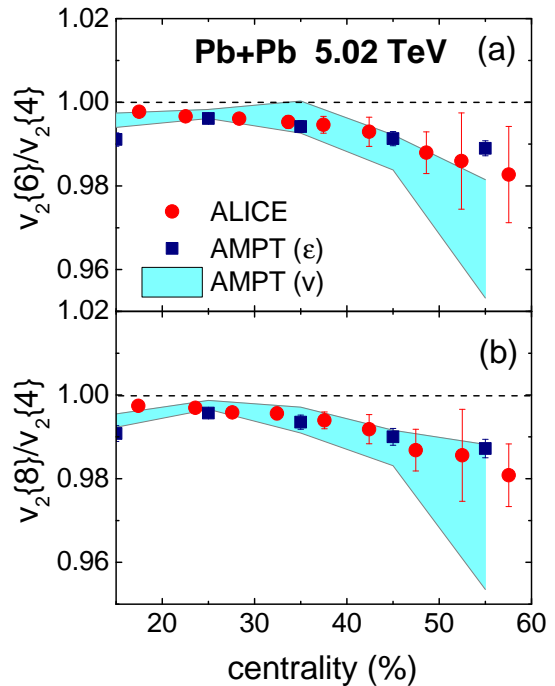


FIG. 7. (Color online) Ratios of cumulants (a)  $v_2\{6\}/v_2\{4\}$  and (b)  $v_2\{8\}/v_2\{4\}$  for Pb-Pb collisions at  $\sqrt{s_{NN}} = 5.02$  TeV. Red points are from ALICE collaboration [22], colored bands are results of AMPT calculations. The corresponding ratios of initial ellipticity  $\varepsilon_2$  are shown as blue squares.

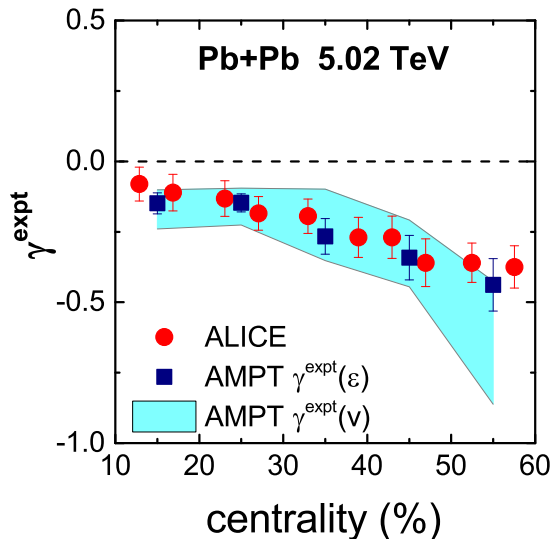


FIG. 8. (Color online) Standardized skewness of  $v_2$  fluctuations in Pb-Pb collisions at  $\sqrt{s_{NN}} = 5.02$  TeV as a function of centrality from AMPT simulations (colored band), and ALICE [22] data (red points). The corresponding results of standardized skewness of initial state  $\varepsilon_2$  are shown as blue squares.

flow signature. Again, the observed fluctuations of  $v_2$  are found compatible with those from initial state  $\varepsilon_2$ , imply-

ing the dominance of linear response relation between  $v_2$  and  $\varepsilon_2$ .

- 
- [1] S. Jeon and U. Heinz, *Int. J. Mod. Phys. E* **24**, 1530010 (2015), [arXiv:1503.03931 \[hep-ph\]](#).
- [2] C. Gale, S. Jeon, B. Schenke, P. Tribedy, and R. Venugopalan, *Phys. Rev. Lett.* **110**, 012302 (2013), [arXiv:1209.6330 \[nucl-th\]](#).
- [3] C. Chattopadhyay, R. S. Bhalerao, J.-Y. Ollitrault, and S. Pal, *Phys. Rev.* **C97**, 034915 (2018), [arXiv:1710.03050 \[nucl-th\]](#).
- [4] S. McDonald, C. Shen, F. Fillion-Gourdeau, S. Jeon, and C. Gale, *Phys. Rev.* **C95**, 064913 (2017), [arXiv:1609.02958 \[hep-ph\]](#).
- [5] H. Niemi, K. J. Eskola, R. Paatelainen, and K. Tuominen, *Phys. Rev.* **C93**, 014912 (2016), [arXiv:1511.04296 \[hep-ph\]](#).
- [6] P. Kovtun, D. T. Son, and A. O. Starinets, *Phys. Rev. Lett.* **94**, 111601 (2005), [arXiv:hep-th/0405231 \[hep-th\]](#).
- [7] J.-Y. Ollitrault, *Phys. Rev.* **D46**, 229 (1992).
- [8] B. Alver and G. Roland, *Phys. Rev.* **C81**, 054905 (2010), [Erratum: *Phys. Rev.* **C82**, 039903 (2010)], [arXiv:1003.0194 \[nucl-th\]](#).
- [9] G. Aad *et al.* (ATLAS), *Phys. Rev.* **C90**, 024905 (2014), [arXiv:1403.0489 \[hep-ex\]](#).
- [10] D. Teaney and L. Yan, *Phys. Rev.* **C83**, 064904 (2011), [arXiv:1010.1876 \[nucl-th\]](#).
- [11] L. Yan, *Chin. Phys.* **C42**, 042001 (2018), [arXiv:1712.04580 \[nucl-th\]](#).
- [12] S. Acharya *et al.* (ALICE), *Phys. Lett.* **B773**, 68 (2017), [arXiv:1705.04377 \[nucl-ex\]](#).
- [13] L. Yan and J.-Y. Ollitrault, *Phys. Lett.* **B744**, 82 (2015), [arXiv:1502.02502 \[nucl-th\]](#).
- [14] G. Giacalone, L. Yan, J. Noronha-Hostler, and J.-Y. Ollitrault, *Phys. Rev.* **C95**, 014913 (2017), [arXiv:1608.01823 \[nucl-th\]](#).
- [15] G. Giacalone, L. Yan, J. Noronha-Hostler, and J.-Y. Ollitrault, *Phys. Rev.* **C94**, 014906 (2016), [arXiv:1605.08303 \[nucl-th\]](#).
- [16] Z.-W. Lin, C. M. Ko, B.-A. Li, B. Zhang, and S. Pal, *Phys. Rev.* **C72**, 064901 (2005), [arXiv:nucl-th/0411110 \[nucl-th\]](#).
- [17] X.-N. Wang and M. Gyulassy, *Phys. Rev. D* **44**, 3501 (1991).
- [18] B. Zhang, *Computer Physics Communications* **109**, 193 (1998).
- [19] J. Xu and C. M. Ko, *Phys. Rev.* **C83**, 034904 (2011), [arXiv:1101.2231 \[nucl-th\]](#).
- [20] Y. Zhang, J. Zhang, J. Liu, and L. Huo, *Phys. Rev. C* **92**, 014909 (2015).
- [21] S. Chatrchyan *et al.* (CMS), *Phys. Rev.* **C87**, 014902 (2013), [arXiv:1204.1409 \[nucl-ex\]](#).
- [22] S. Acharya *et al.* (ALICE), (2018), [arXiv:1804.02944 \[nucl-ex\]](#).
- [23] J. Adam *et al.* (ALICE), *Phys. Rev. Lett.* **116**, 132302 (2016), [arXiv:1602.01119 \[nucl-ex\]](#).
- [24] A. M. Sirunyan *et al.* (CMS), (2017), [arXiv:1711.05594 \[nucl-ex\]](#).
- [25] J. Noronha-Hostler, L. Yan, F. G. Gardim, and J.-Y. Ollitrault, *Phys. Rev.* **C93**, 014909 (2016), [arXiv:1511.03896 \[nucl-th\]](#).
- [26] F. G. Gardim, F. Grassi, M. Luzum, and J.-Y. Ollitrault, *Phys. Rev.* **C85**, 024908 (2012), [arXiv:1111.6538 \[nucl-th\]](#).
- [27] D. Solanki, P. Sorensen, S. Basu, R. Raniwala, and T. K. Nayak, *Phys. Lett.* **B720**, 352 (2013), [arXiv:1210.0512 \[nucl-ex\]](#).
- [28] J. Xu and C. M. Ko, *Phys. Rev.* **C84**, 014903 (2011), [arXiv:1103.5187 \[nucl-th\]](#).
- [29] S. Chatrchyan *et al.* (CMS), *Phys. Rev.* **C89**, 044906 (2014), [arXiv:1310.8651 \[nucl-ex\]](#).
- [30] S. Acharya *et al.* (ALICE), (2018), [arXiv:1805.04390 \[nucl-ex\]](#).
- [31] G. Aad *et al.* (ATLAS), *Eur. Phys. J.* **C74**, 3157 (2014), [arXiv:1408.4342 \[hep-ex\]](#).